Polymer Chemistry

SUPPLEMENTARY INFORMATION for

Spatial control of surface topography in photo-sensitive block copolymer films

Lewis C. Chambers,† Yun Huang,† Kevin S. Jack,‡ Idriss Blakey,†,§*

The University of Queensland, †Australian Institute of Bioengineering and Nanotechnology, ‡Centre for Microscopy and Microanalysis, §Centre for Advanced Imaging, Brisbane, QLD, Australia, 4072

Instrumentation. All ^{1}H NMR spectra were collected on a Bruker Ascend spectrometer with an operating frequency of 400 MHz at 298 K. All samples were referenced against the peak of residual $CHCl_3$ at 7.26 ppm or DMSO at 2.5 ppm. Size Exclusion Chromatography (SEC) was performed using a Waters Alliance 2690 Separations Module equipped with a 717 autosampler, column heater, 1515 isocratic pump, 2414 differential refractive index detector and a photodiode array. HPLC grade THF was used as the eluent at a flow rate of 1 mL min^{-1}. The three columns were 7.8 x 300 mm Waters Styragel SEC columns connected in series, two linear Ultra Styragel and one Styragel HR3 column. The system was calibrated with an 11-point standard curve constructed with PS standards. Differential Scanning Calorimetry (DSC) was performed on a Mettler Toledo STAR^{e} DSC system under a nitrogen atmosphere with a nitrogen flow rate of 30 cm^3 min^{-1}. Samples were heated from room temperature to 250 °C at 20 °C min^{-1}, cooled to – 50 °C at 50 °C min^{-1} and held there for 30 min. This heat/cool cycle was repeated twice. The data presented here is taken from the second heating cycle. Thermogravimetric Analysis (TGA) was performed on a Mettler Toledo STAR^{e} TGA/DSC system under a nitrogen atmosphere with a nitrogen flow rate of 10 cm^3 min^{-1}. Samples were heated from room temperature to 120 °C at 10 °C min^{-1} and held at that temperature for 10 h. Small Angle X-ray Scattering samples were prepared by dissolving ~ 5 mg of polymer in a minimum amount of THF and drop casting into 0.5 x 0.5 mm cylindrical wells backed with Kapton tape. Samples were annealed at 190 °C for 16 h under vacuum and then sealed with Kapton tape on top. Block copolymer morphology in bulk and in thin films was characterized through small angle x-ray scattering (SAXS) and grazing incidence small angle x-ray scattering (GISAXS) on the Australian Synchrotron SAXS/WAXS beamline. The beamline was configured with an X-

ray wavelength of 1.033201 Å (12.000002 keV) and focused to a 250 µm x 150 µm vertical spot. Two dimensional (2D) scattering patterns were measured on a Dectris-Pilatus 1M detector with a size of 169 x 179 mm and a sample to detector distance of 1.6 m. The 2D scattering patterns were radially integrated to give one dimensional scattering profiles which were plotted as intensity (I) multiplied by the wave vector (q) squared versus the wave vector, $q = 4\pi \sin(\theta/2)/\lambda$ where θ is the scattering angle and λ is the X-ray wavelength. GISAXS scattering patterns were collected with the beam striking the surface of the sample at an angle of 0.10° and an exposure time of 10 s, unless otherwise specified. The 2D scattering patterns were summated vertically from $q_z = 0.039 – 0.043$ Å^{-1} to give one dimensional scattering profiles were plotted as log(I) vs. log(q_{xy}). The full width half maximum was calculated by fitting a Lorenztian function to the scattered peak. Film thicknesses were measured via ellipsometry on a J.A Woollam M-2000 spectroscopic ellipsometer. Measurements were taken at 5 angles (55, 60, 65, 70, 75°) between at energies between 450 and 1000 nm. Film thickness was calculated by modelling the sample as a Cauchy layer on a silicon wafer with a native silicon oxide layer and fitting the model to the data. Grazing Angle Attenuated Total Reflectance Fourier Transform Infrared (GA-ATR FTIR) spectra were collected on a Nicolet Nexus 5700 FTIR spectrometer equipped with a Harrick single reflection ATR accessory with a Germanium crystal and an angle of incidence of 65°. Spectra were collected as the average of 128 interferograms between 4000 and 650 cm^{-1} with a resolution of 4 cm^{-1} before a Fourier Transformation was applied. Atomic Force microscopy (AFM) was performed on an Asylum Research Cypher Scanning Probe Microscope operating in tapping mode in air. The AFM was mounted on an anti-vibration table (Table Stable Ltd.). Height and phase images were captured at 512 points per line at 1 Hz. Etalon cantilevers (resonant frequency 140 kHz, spring constant 3.5 N m^{-1}, radius of curvature < 10 nm) were obtained from NT-MDT Spectrum Instruments.

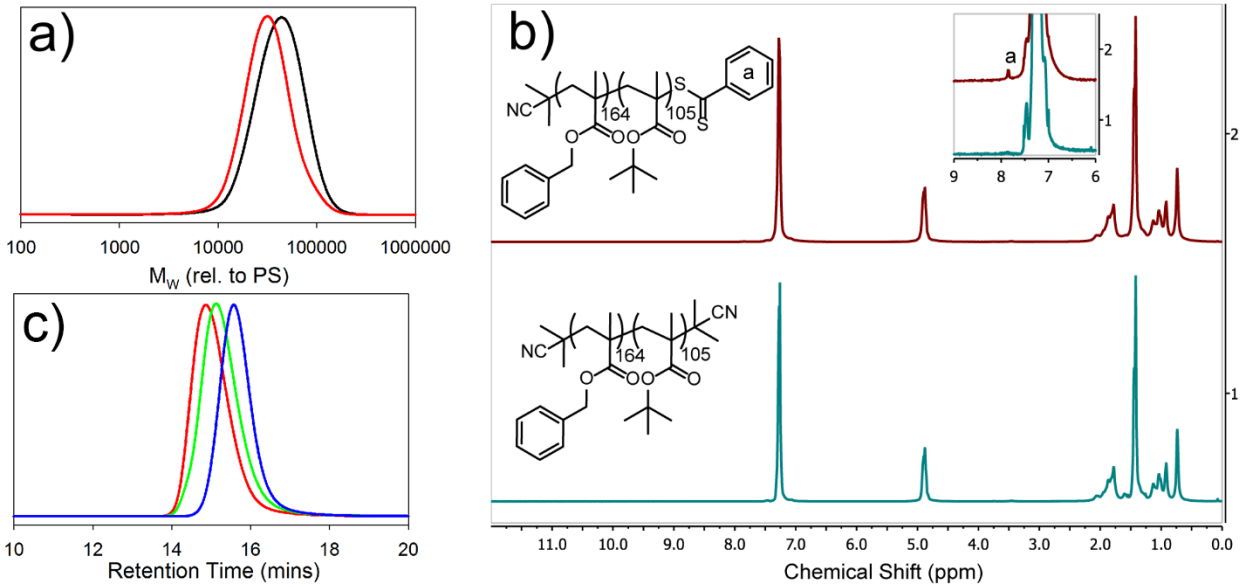

Figure S1: a) SEC traces of PBnMA$_{164}$-*block*-PtBMA$_{105}$ before (black) and after (red) RAFT end group cleavage, showing no chain coupling. b) ^{1}H NMR of PBnMA$_{164}$-*block*-PtBMA$_{105}$ before (top) and after (bottom) RAFT end group cleavage, with the inset showing the loss of the RAFT phenyl group. c) Raw SEC chromatograms of PBnMA$_{164}$ (blue) and PBnMA$_{164}$-*block*-PtBMA$_{105}$ before (green) and after (red) RAFT end group cleavage

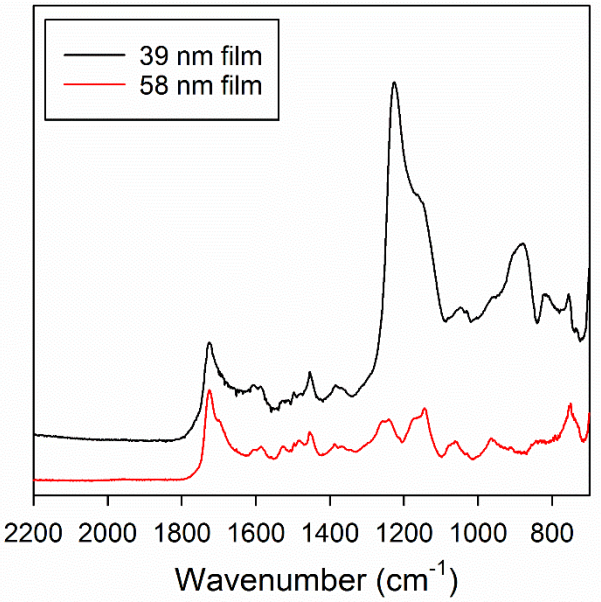

Figure S2: IR spectra of $PBnMA_{164}$-*block*-($PNBMA_{87}$-*ran*-$PMAA_{18}$) films, 39 nm (black) and 58 nm (red) thick after exposure to 2000 mJ cm^{-2} of light from a broadband UV source. Spectra were acquired using GA-ATR.

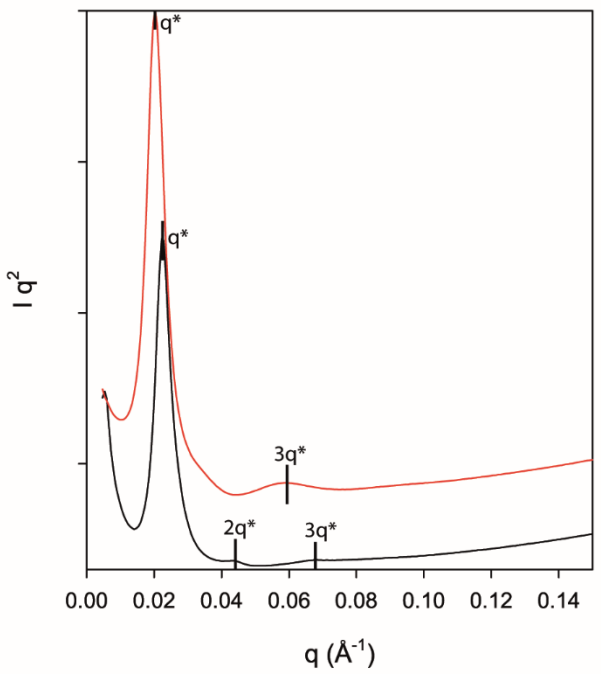

Figure S3: SAXS pattern of $PBnMA_{164}$-*block*-($PNBMA_{87}$-*ran*-$PMAA_{18}$) (black) and $PBnMA_{164}$-*block*-$PMAA_{105}$ (red), with higher order reflections indicating a lamellar morphology marked.

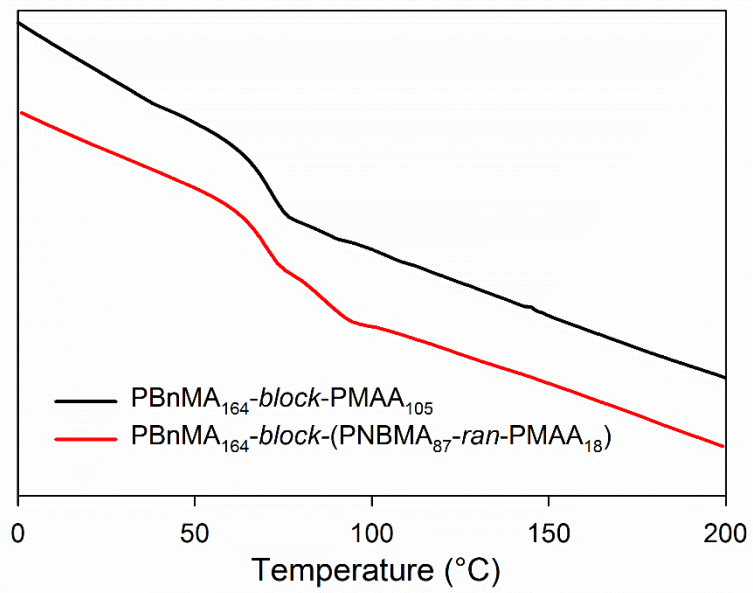

Figure S4: a) DSC traces of $PBnMA_{164}$-*block*-($PNBMA_{87}$-*ran*-$PMAA_{18}$) and b) $PBnMA_{164}$-*block*-$PMAA_{105}$ obtained on the 3rd heating cycles. a) shows the T_g of PBnMA at 68.3 °C and of $PNBMA_{87}$-*ran*-$PMAA_{18}$ at 89.5 °C, while b) shows only the T_g of PBnMA.

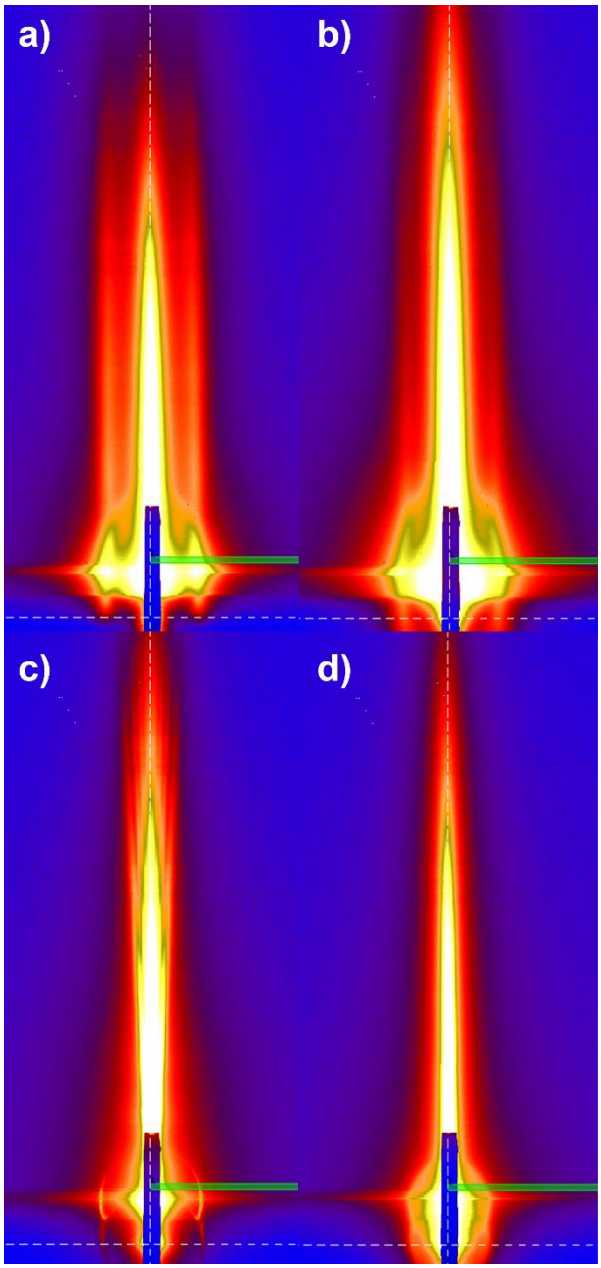

Figure S5: GISAXS Scattering patterns for a) an as-cast film of $PBnMA_{164}$-*block*-($PNBMA_{87}$-*ran*-$PMAA_{18}$), b) an irradiated film, c) and non-irradiated film that has been annealed at 120 °C and d) an irradiated film that has been annealed at 120 °C. The dotted white lines in each image indicate where q_{xy} and $q_z = 0$. To produce the 1D scattering profiles presented in Figure 3, these images where summated vertically in the area indicated by the partially transparent green box, from $q_z = 0.039 - 0.043$ Å^{-1}.

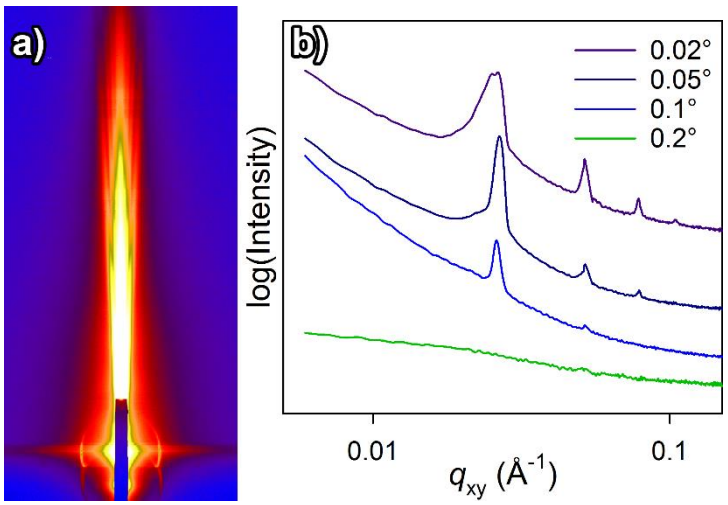

Figure S6: a) 2D GISAXS scattering pattern on a non-irradiated annealed film obtained at 0.1°. The sharp, partial rings around the transmitted and reflected beams indicate the presence of some perpendicular structures, while the flaring indicates the formation of terraces driven by parallel structures b) 1D GISAXS patterns of a non-irradiated annealed film collected at different angles of incidence. The 1D traces were obtained by summating the 2D patterns vertically over a range of 0.0086 Å^{-1} just below the Yoneda line and projected onto the q_{xy} plane. The intensity of the peaks drops away as the angle of incidence is increased, suggesting that the perpendicular structures are localised at the film surface.

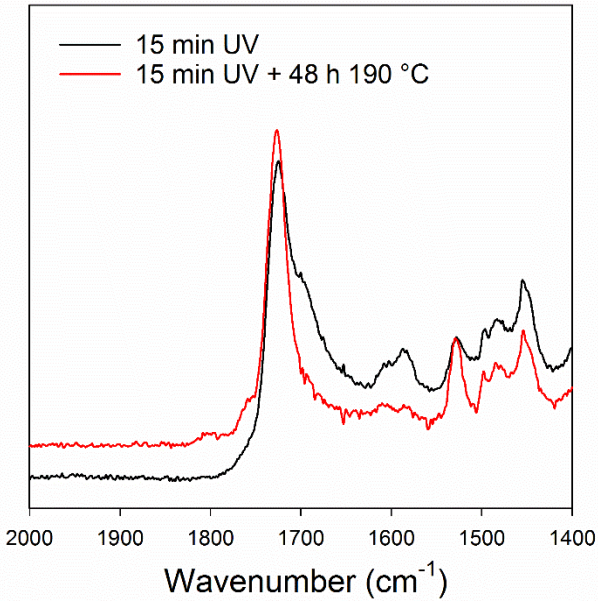

Figure S7: IR spectra of films acquired via GA-ATR. The thermally annealed film (red) displays an extra peak at 1810 cm^{-1} and a shoulder at 1760 cm^{-1} which are characteristic of anhydrides and are not present prior to thermal annealing (black).[1]

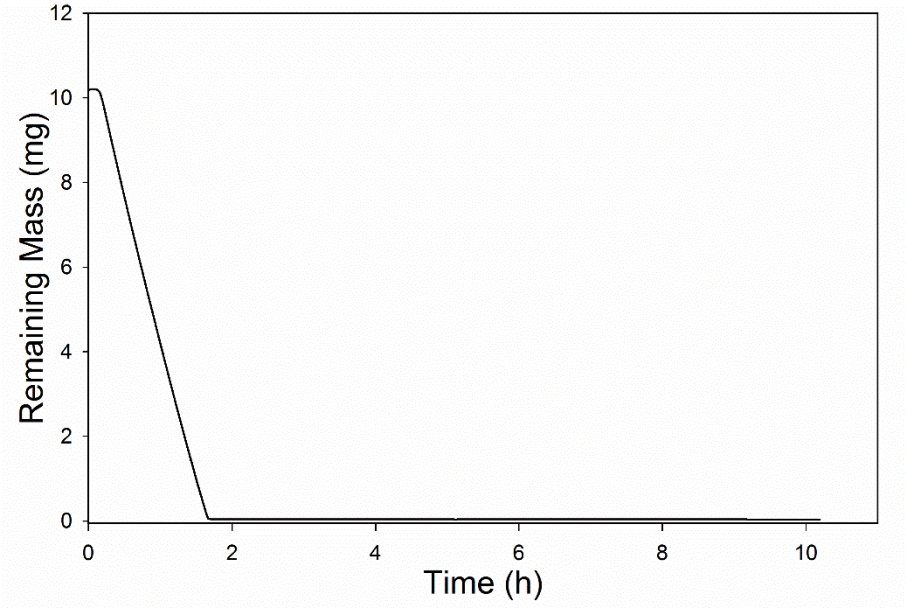

Figure S8: Thermal Gravimetric Analysis of *o*-nitrobenzaldehyde which was analysed as an analogue of the side-product of photo-deprotection, *o*-nitrosobenzaldehyde. 10 mg of material was heated from 25 °C to 120 °C at 10 °C min^{-1}, then held at 120 °C for 10 h. After 1.6 h the sample had completely evaporated.

2

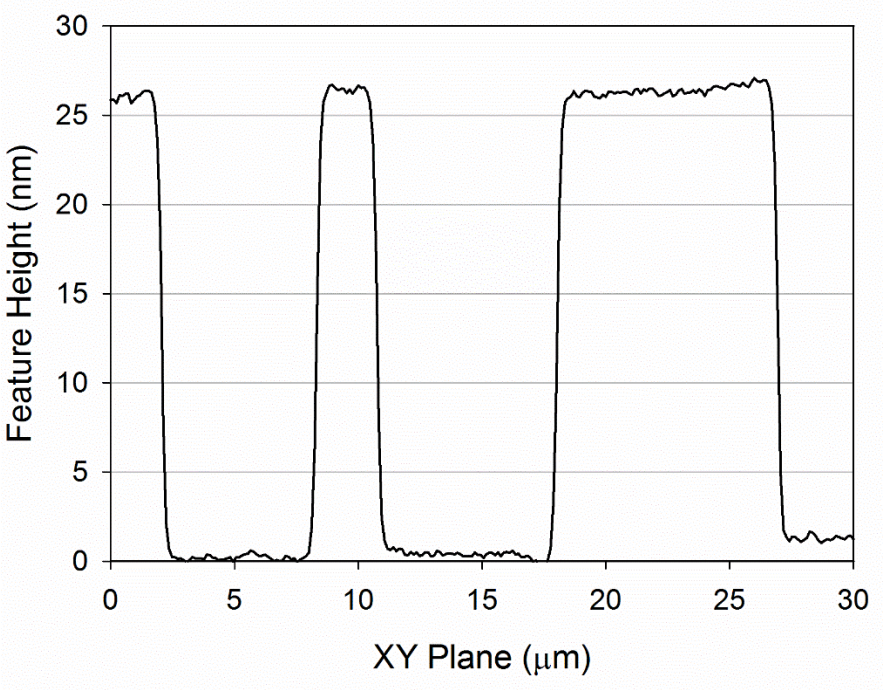

Figure S9: Height trace obtained from an AFM Height image. From this trace, the $L_{0,TF}$ of the film was measured to be 26 ±2 nm.

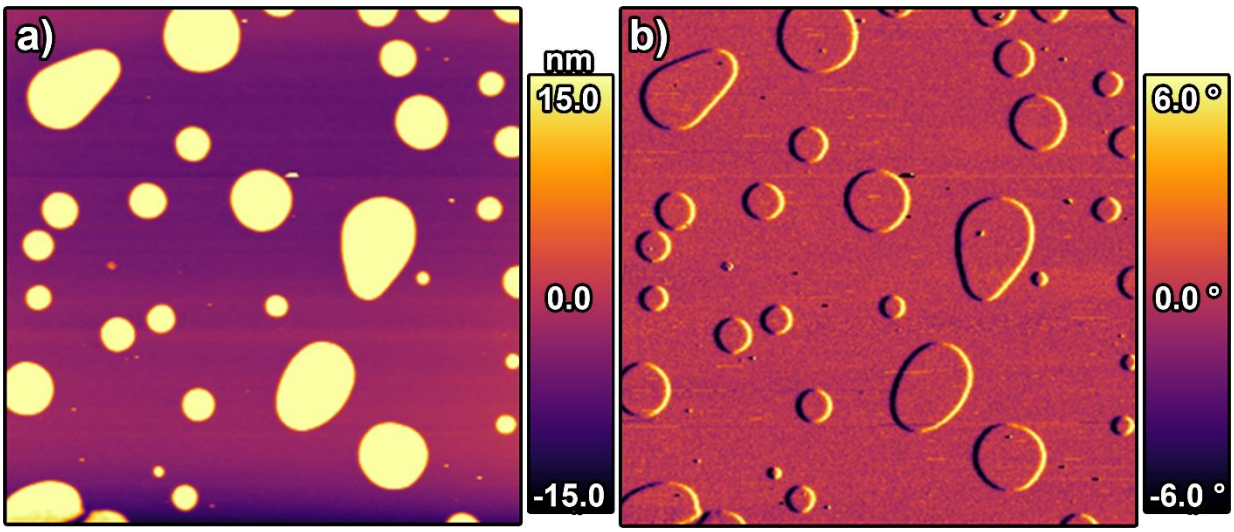

Figure S10: AFM Height (a) and Phase (b) images of the same area of a $PBnMA_{164}$-*block*-($PNBMA_{87}$-*ran*-$PMAA_{18}$) film following annealing at 120 °. AFM Phase imaging can offer contrast between areas of different mechanical properties across a surface and is often used in the characterisation of block copolymer films to distinguish between different domains when such a contrast exists. The lack of contrast between the two levels of the terrace structure is consistent with the PBnMA block wetting the air interface across the entire film surface.

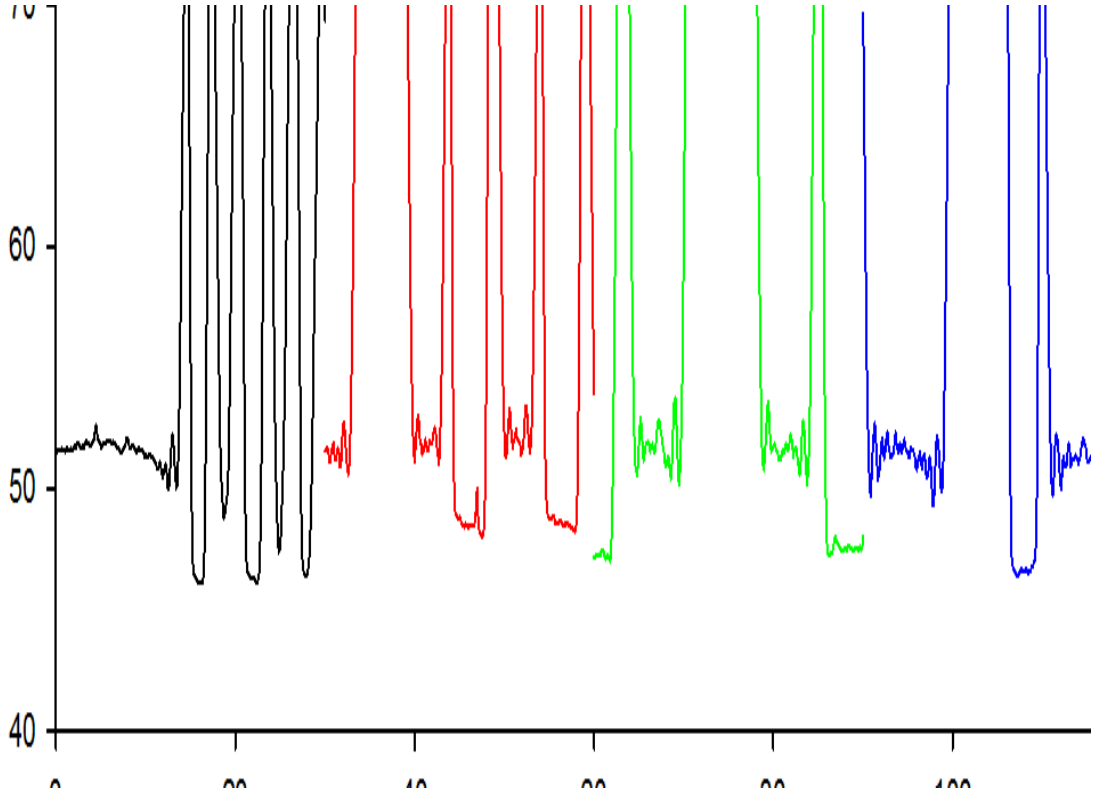

Figure S11: Height traces of a 51.8 nm thick film bearing 3, 5, 7 and µm features. Regardless of feature size, the film thickness in the non-irradiated regions is seen to quantize to roughly the same film thicknesses.

Estimating Change in Molar Volume after Photo-deprotection. To estimate the change in molar volume that could occur when *o*-nitrosobenzaldehyde is cleaved off and evaporates, the change in molar volume between its protected and deprotected forms was calculated. The molar volume of the polymer was estimated as the sum of the molar volumes of the monomers that it is composed of. The molar volumes of BnMA and MAA were obtained from the NIMS PolyInfo database,[2] which calculates the molar volume as 1.6 times the Van Krevelen's Van der Waals volume. For NBMA no molar volume could be found in the database, so it was estimated as the molar volume of BnMA plus the molar volume of 2-nitrophenyl methacrylate minus the molar volume of phenyl methacrylate (ie. the molar volume of just the nitro group).

Before Deprotection				After Deprotection				Volume Loss (cm^3 mol^{-1})	Volume Loss (%)
Monomer	DP	Monomer Molar Volume (cm^3 mol^{-1})	Polymer Molar Volume (cm^3 mol^{-1})	Monomer	DP	Monomer Molar Volume (cm^3 mol^{-1})	Polymer Molar Volume (cm^3 mol^{-1})		
B*n*MA	164	157.6	25846.4	B*n*MA	164	157.6	25846.4		
MAA	18	69.92	1258.56	MAA	105	69.92	7341.6		
NBMA	87	180.4	15694.8						
TOTAL			42799.76	TOTAL			33188	9612	22.5

Measuring Change in Film Thickness after Photo-deprotection

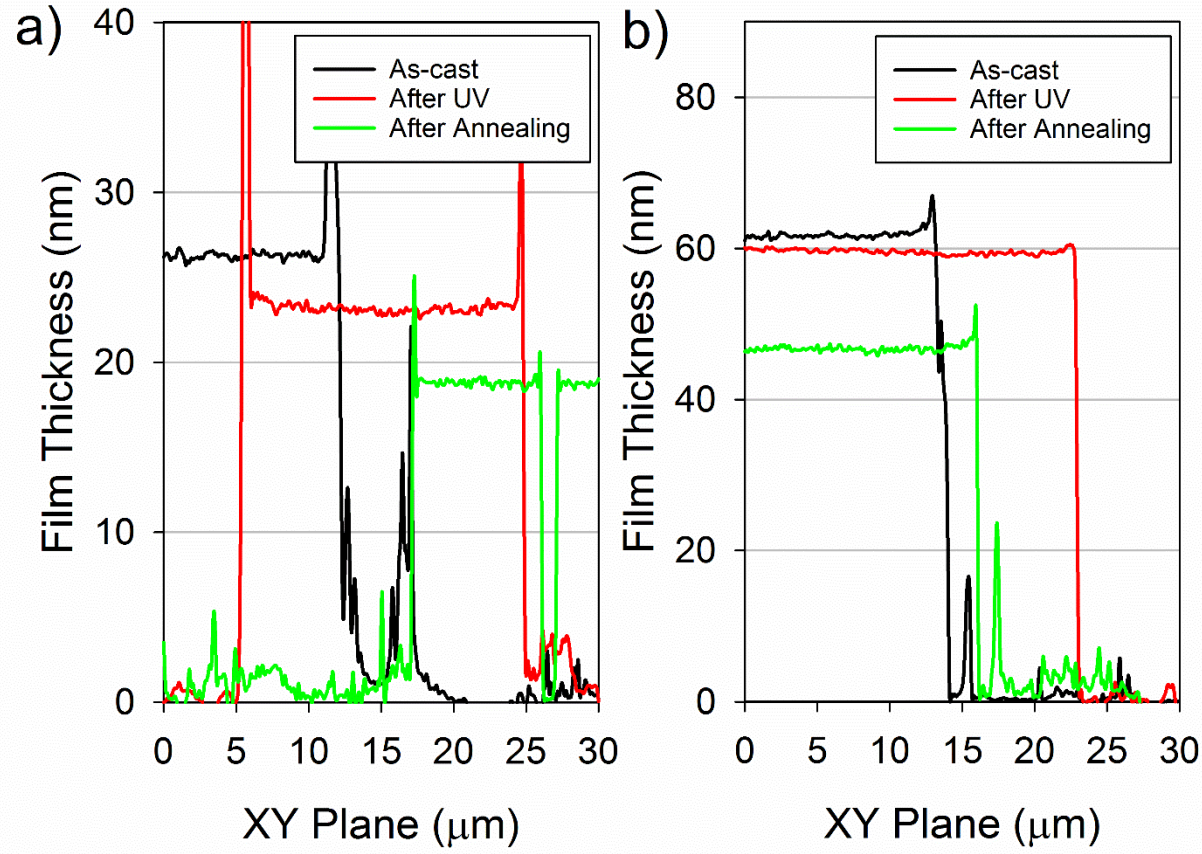

Figure S12: Height profile of a thin film from an AFM scratch test before UV exposure (as-cast, 26.1 nm thick), after UV exposure (23.0 nm, 3.1 nm or 11.6 % thinner) and after UV exposure and 48 h thermal annealing at 120 °C (18.6 nm thick, 7.5 nm or 28.7 % thinner). b) Height profile of a thick film from an AFM scratch test before UV exposure (as-cast, 61.8 nm thick), after UV exposure (59.6 nm, 2.2 nm or 3.5 % thinner) and after UV exposure and 48 h thermal annealing at 120 °C (47.2 nm thick, 14.6 nm or 23.6 % thinner).

After UV exposure, both films experience similar absolute decreases in thickness but different decreases in their relative thickness. This is likely because evaporation of the deprotection side product is limited by its diffusion to the surface, so evaporation of this species only occurs from a relatively thin layer closest to the film surface. After thermal annealing of UV treated films, the decreases

in relative thickness are more similar as the elevated temperature promotes diffusion of the deprotection side product to the surface and its subsequent evaporation.

A 22.5 % volume loss would correspond to an 8.1 % decrease in thickness if the polymer film was free to contract along all dimensions. However, adhesive interactions between the polymer and the substrate likely frustrate contraction in the plane of the film, leaving vertical contraction to account for more of the volume loss. Additionally, relaxation of the chains from a non-equilibrium conformation after spin coating and the evaporation of any residual spin coating solvent may also contribute to the measured film thickness reduction.

Analysis of Buckling Wavelength. According to the work of Volynskii et. al.[3] the wavelength of the buckling pattern of a thin, rigid film on a rubbery substrate can be predicted as a function of the film thickness and the ratio of the elastic moduli of the two layers through the following relationship:

$$\lambda = 2\pi h \sqrt[3]{\frac{(1-v_1^2)E_2}{3(1-v_2^2)E_1}}$$

where h is the thickness of the rigid layer, υ_1 and υ_2 represent the Poisson's ratios of the rubbery and rigid phases respectively, and E_1 and E_2 represent the elastic moduli of the rubbery and rigid phases respectively. The Poisson's ratio of the glassy PMAA was modelled as that of glassy PMMA (0.371) and the Poisson's ratio of the rubbery PBnMA was taken as 0.5, as is common of polymers above their T_g.[4] The thickness of the rigid layer h was taken as 0.5 L_0, 12.8 nm. Based on these figures and the measured λ of 1 µm, E_2/E_1 was calculated to be ~5,000, which is in the range estimated for a glassy and rubbery polymer.

It should be noted that the model established by Volynskii et. al. considered a system composed of a thin rigid layer on top of an elastomeric substrate, where the thickness of the rubbery layer is much greater than that of the rigid layer. In the system analyzed here, the thickness of the two layers is roughly equal. This may introduce an added layer of uncertainty to the final value, in addition to the various estimation of the Poisson's ratio. As such, the value presented here serves to show the plausibility of the hypothesised buckling mechanism as an explanation of the observed patterns in the exposed regions of the surface and a more rigorous analysis would be required to fully characterize the phenomenon.

1. Ho, B. C.; Lee, Y. D.; Chin, W. K., *J. Polym. Sci. Pol. Chem.* **1992,** *30*, 2389-2397.
2. Polymer Database. https://polymer.nims.go.jp/index_en.html (accessed 20/09/2018).
3. Volynskii, A. L.; Bazhenov, S.; Lebedeva, O. V.; Bakeev, N. F., *J. Mater. Sci.* **2000,** *35*, 547-554.
4. Seitz, J. T., *J. Appl. Polym. Sci.* **1993,** *49*, 1331-1351.

